Reduction of the Ordered Magnetic Moment by Quantum Fluctuation in the Antiferromagnetic Spin-$\frac{5}{2}$ Dimer Compound $FeVMoO_7$

Masashi Hase[1]*, James R. Hester[2], Kirrily C. Rule[2], Vladimir Yu. Pomjakushin[3], Akira Matsuo[4], and Koichi Kindo[4]

[1]*Research Center for Advanced Measurement and Characterization, National Institute for Materials Science (NIMS), 1-2-1 Sengen, Tsukuba-shi, Ibaraki 305-0047, Japan*

[2]*Australian Nuclear Science and Technology Organisation (ANSTO), Locked Bag 2001, Kirrawee DC NSW 2232, Australia*

[3]*Laboratory for Neutron Scattering and Imaging, Paul Scherrer Institut (PSI), CH-5232 Villigen PSI, Switzerland*

[4]*The Institute for Solid State Physics (ISSP), The University of Tokyo, 5-1-5 Kashiwanoha, Kashiwa-shi, Chiba 277-8581, Japan*

We investigated the magnetism of $FeVMoO_7$ by performing magnetization, specific heat, electron spin resonance, and neutron diffraction experiments. We observed an antiferromagnetically ordered state below $T_N = 10.8$ K. We consider that the probable spin model is an interacting antiferromagnetic spin-$\frac{5}{2}$ dimer model where spin dimers are connected by interdimer interactions. The intradimer interaction was evaluated to be $J = 10.5 \pm 0.5$ K. The magnitude of ordered magnetic moments is $4.00(7)\mu_B$ at 4 K. The magnitude at 0 K is considered to be smaller than the classical value $4.95\mu_B$ ($g = 1.98$). We confirmed a reduction of ordered magnetic moments by quantum fluctuation in high-spin (spin-$\frac{5}{2}$) clusters as known in high-spin chains.

1. Introduction

Antiferromagnetic (AF) XXZ models describe the competition between quantum and classical nature. The Hamiltonian is expressed as

$$\mathcal{H} = \sum_{i,j} J_{ij}\left(\frac{S_{i+}S_{j-} + S_{i-}S_{j+}}{2} + \Delta S_{iz}S_{jz}\right). \quad (1)$$

*HASE.Masashi@nims.go.jp

The first term in the parentheses stabilizes spin-singlet pairs, induces quantum fluctuation, and destroys magnetic long-range order, whereas the second term stabilizes magnetic long-range order. In low-spin systems, we know examples where quantum fluctuation prevails over magnetic long-range order such as the spin-Peierls transition (spin-$\frac{1}{2}$)[1–3] and the Haldane gap (spin-1).[4–6] This Hamiltonian is valid regardless of the magnitude of the spin. Therefore, quantum nature can exist in high-spin systems such as spin-$\frac{5}{2}$.

A Heisenberg model can explain the magnetism of the AF spin-$\frac{5}{2}$ trimer compound $SrMn_3P_4O_{14}$ where the Hamiltonian is $\mathcal{H} = J(S_1 \cdot S_2 + S_2 \cdot S_3)$.[7–11] We evaluated a magnetic-field-induced magnetic moment on each Mn^{2+} site in the 1/3 quantum magnetization plateau ground state (GS) using neutron diffraction.[11] In the GS, quantum mechanical values are calculated as $S_{1z} = S_{3z} = \frac{15}{7}$ and $S_{2z} = -\frac{25}{14}$, whereas classical values are $S_{1z} = S_{3z} = \frac{5}{2}$ and $S_{2z} = -\frac{5}{2}$. Experimental values obtained from neutron diffraction measurements agree well with the quantum mechanical values. Consequently, we have concluded that the spin-$\frac{5}{2}$ in $SrMn_3P_4O_{14}$ can be considered a quantum spin.

We can see quantum fluctuation in high-spin chains and clusters. The GS can be a spin-singlet state in these spin systems. For example, in a uniform chain with only nearest-neighbor AF interactions, the GS is a Tomonaga-Luttinger liquid and a valence-bond-solid state[6] for half odd integer and integer spins, respectively. The GS of the spin dimer is also a spin-singlet state. A magnetically ordered state can appear by the introducing interchain and intercluster interactions. The ordered magnetic moment is expected to shrink owing to the effect of the singlet GS. Table I shows results of spin-chain and spin-cluster compounds having spin-$\frac{5}{2}$. Reduced moments were observed in these compounds, indicating that quantum fluctuation exists.

There are not many experimental results that show quantum fluctuations resulting in a reduced magnetic moment in high-spin clusters. Further experimental confirmation of quantum fluctuations is therefore important. In this work, we focus our attention on the spin-$\frac{5}{2}$ compound $FeVMoO_7$.[19,20] Figure 1 shows the unit cell of the crystal structure of $FeVMoO_7$. Fe^{3+} ions ($3d^5$) possess a localized spin-$\frac{5}{2}$. The shortest distance between two Fe^{3+} ions is 3.11 Å at 153 K, whereas the other Fe-Fe distances are 5.01 Å or longer.[20] If the exchange interaction in the shortest Fe-Fe pair is dominant and AF, the spin system in $FeVMoO_7$ consists of AF spin dimers. We studied the magnetism of $FeVMoO_7$ powder by performing magnetization, specific heat, electron spin resonance, and neutron diffraction experiments. We report the results in this paper.

Table I. Magnitude of ordered magnetic moments (m) in spin-chain and spin-cluster compounds having spin-$\frac{5}{2}$. This table also shows the temperature at which the magnitude of ordered magnetic moments was determined ($T_{\rm mea}$), the AF transition temperature ($T_{\rm N}$), and the temperature at which the magnetic susceptibility shows a maximum ($T_{\rm max}$). In $Cu_2Fe_2Ge_4O_{13}$, Fe^{3+} and Cu^{2+} ions have spin-$\frac{5}{2}$ and spin-$\frac{1}{2}$, respectively. The spin tetramers Fe-Cu-Cu-Fe are formed. The probable spin model in $FeVMoO_7$ is an interacting AF spin-$\frac{5}{2}$ dimer model where spin dimers are connected by interdimer interactions.

	m ($\mu_{\rm B}$)	$T_{\rm mea}$ (K)	$T_{\rm N}$ (K)	$T_{\rm max}$ (K)	Ref.
classical value	~ 5				
chain					
$SrMn(VO_4)(OH)$	3.4(1)	4	30	80	[12]
$BaMn_2Si_2O_7$	3.9	4	26	55	[13]
$SrMn_2V_2O_8$	3.99(1)	1.5	42.2(2)	170	[14]
$NaFeGe_2O_6$	4.09(4)	2.5	11.2	33.8	[15]
$LiFeGe_2O_6$	4.48(5)	5	20.2(2)	24.4(2)	[16]
cluster					
$Cu_2Fe_2Ge_4O_{13}$	3.62(3) Fe	1.5	39	100	[17,18]
	0.38(4) Cu				
$FeVMoO_7$	4.00(7)	4	10.8	16	this work

2. Experimental and Calculation Methods

Crystalline $FeVMoO_7$ powder was synthesized by a solid-state reaction. The starting materials were Fe_2O_3 (purity 99.9%), V_2O_5 (99.99%), and MoO_3 (99.99%) powders. A stoichiometric mixture of the powders was sintered at 903 K in air for 88 h in total. An X-ray powder diffraction pattern was measured at room temperature using an X-ray diffractometer (RINT-TTR III, Rigaku). We detected only reflections of $FeVMoO_7$. This leads us to believe that our sample is a single phase of $FeVMoO_7$ within experimental accuracy.

Electron spin resonance (ESR) measurements were carried out using an X-band spectrometer (JES-FE2XG, JEOL) at room temperature. We performed specific heat measurements and magnetization measurements in magnetic fields of up to 5 T using a physical property measurement system (Quantum Design) and a superconducting quantum interference device magnetometer (magnetic property measurement system, Quantum Design), respectively. High-field magnetization measurements were carried out using an induction method with a multilayer pulsed field magnet at the Institute for Solid State Physics (ISSP), The University of Tokyo.

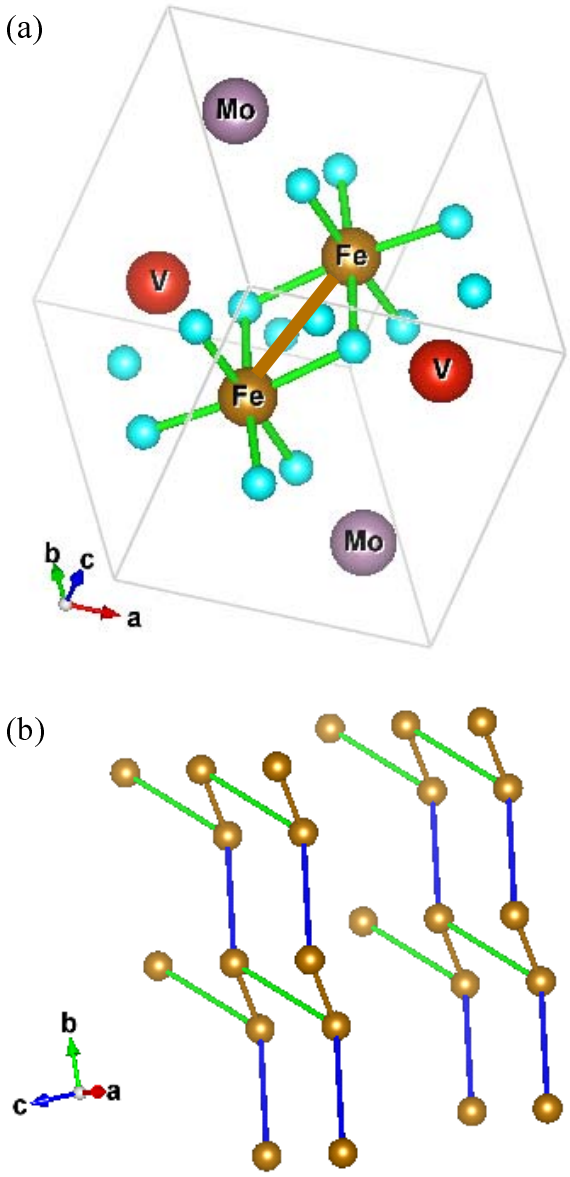

Fig. 1. (Color online) (a) Unit cell of $FeVMoO_7$.[19,20] The brown line indicates the shortest Fe-Fe pair (3.11 Å at 153 K).[20] (b) Schematic figure showing Fe positions. The brown, green, and blue lines indicate the shortest pairs, the second shortest pairs (5.01 Å), and the third shortest pairs (5.32 Å), respectively.

Neutron powder diffraction experiments were performed using the high-resolution powder diffractometer ECHIDNA (Proposal ID MI7075) at the Open Pool Australian Lightwater (OPAL) reactor at Australian Nuclear Science and Technology Organisation (ANSTO). We carried out Rietveld refinements of the crystal and magnetic structures using the `FULLPROF SUITE` program package[21] with its internal tables for scattering lengths and magnetic form factors.

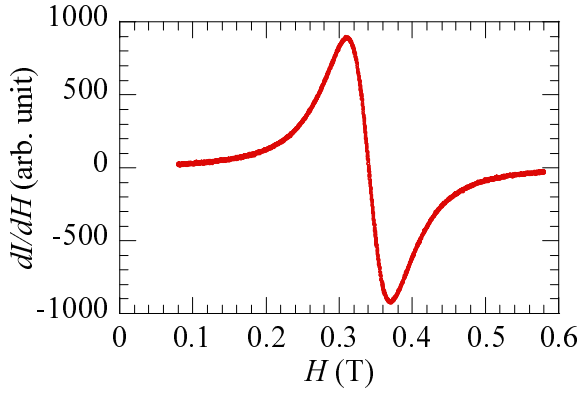

Fig. 2. (Color online) Electron paramagnetic resonance (EPR) spectrum of $FeVMoO_7$ powder at room temperature measured using an X-band electron spin resonance (ESR).

The eigenenergies of an isolated spin-$\frac{5}{2}$ dimer were calculated using an exact diagonalization method. We calculated the temperature T dependence of the magnetic susceptibility $\chi(T)$ and the magnetic-field H dependence of the magnetization $M(H)$ using the eigenenergies.

3. Results

3.1 Results obtained by bulk methods

We show the H derivative of the intensity of the electron paramagnetic resonance (EPR) of the $FeVMoO_7$ powder at room temperature in Fig. 2. The frequency (f) of the incident microwave is 9.442 GHz. We observed a clear resonance. The intensity (I) shows a maximum at around $H_{\rm r} = 0.341$ T where $dI/dH = 0$. From the relation $g = \frac{hf}{\mu_{\rm B} H_{\rm r}}$, the g value was evaluated to be 1.98 ± 0.02.

We show the T dependence of the specific heat divided by T $[C(T)/T]$ of an $FeVMoO_7$ pellet in zero magnetic field and the T derivative of the magnetic susceptibility $[d\chi(T)/dT]$ of $FeVMoO_7$ powder in $H = 0.1$ T in Fig. 3(a). A λ-type peak typical of the second-order phase transition was observed in both measurements at around 10.8 K. The peak indicates an AF transition. As described later, an antiferromagnetically ordered state was observed at low T in neutron powder diffraction experiments.

We show the T dependence of $\chi(T)$ of the $FeVMoO_7$ powder in $H = 0.1$ T by the red circles in Fig. 3(b). The broad maximum of $\chi(T)$ around 16 K indicates a low-dimensional AF spin system with short-range correlations. The susceptibility appears to approach a finite value (~ 0.04 emu/mol Fe) at 0 K. The magnetic order generates

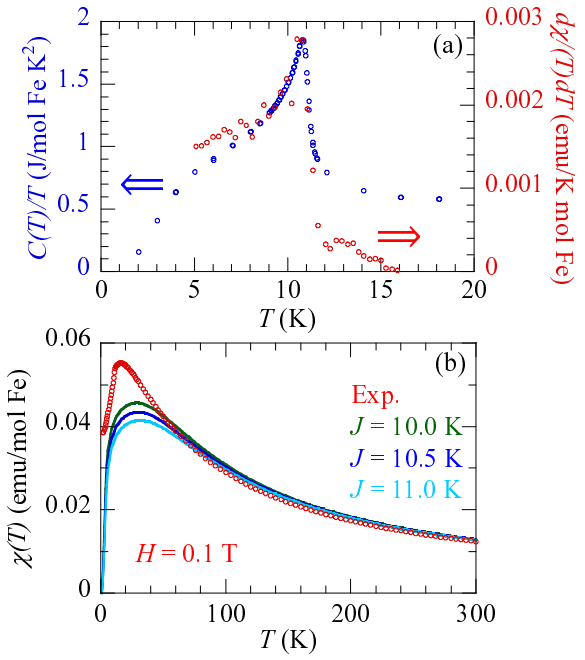

Fig. 3. (Color online) (a) Temperature (T) dependence of the specific heat divided by T [$C(T)/T$] of $FeVMoO_7$ in zero magnetic field and T derivative of the magnetic susceptibility [$d\chi(T)/dT$] of $FeVMoO_7$ in a magnetic field of $H = 0.1$ T. (b) T dependence of $\chi(T)$ of $FeVMoO_7$ in $H = 0.1$ T (red circles). The lines indicate $\chi(T)$ calculated for the isolated AF spin-$\frac{5}{2}$ dimers with $J = 10.0$ K (green), 10.5 K (blue), and 11.0 K (lightblue). We used $g = 1.98$ determined in the EPR measurement.

finite susceptibility at 0 K. We fitted the formula $\frac{C}{T+T_W} + \chi_0$ to the susceptibility. We used $C = 4.29$ (emu K/mol Fe) obtained from the spin value $S = \frac{5}{2}$ and $g = 1.98$. We evaluated $T_W = 47$ K and $\chi_0 = 5.0 \times 10^{-5}$ (emu/mol Fe) from the susceptibility above 200 K. The values are nearly independent of the T range of the fitting. The value of T_W is close to 51[20] and 49 K.[22,23] The susceptibility obtained in this result is close to that reported for the supporting material in the literature.[20] Groń et al.[22] and Kurzawa[23] reported the T dependence of $1/\chi(T)$ above 77 K and the magnetization above 4.2 K, respectively. Wang et al.[20] and we observed the broad maximum around 16 K in $\chi(T)$ in 0.1 T, whereas Kurzawa observed a peak at 14 K in the magnetization in 10 T. The different T dependences are probably caused by the different magnetic fields.

We show the H dependence of the magnetization [$M(H)$] of the $FeVMoO_7$ powder measured at 4.2 and 1.3 K by the red and pink lines, respectively, in Fig. 4. As the magnetic field increases, the magnetizations increase monotonically and seem to approach saturation above 40 T.

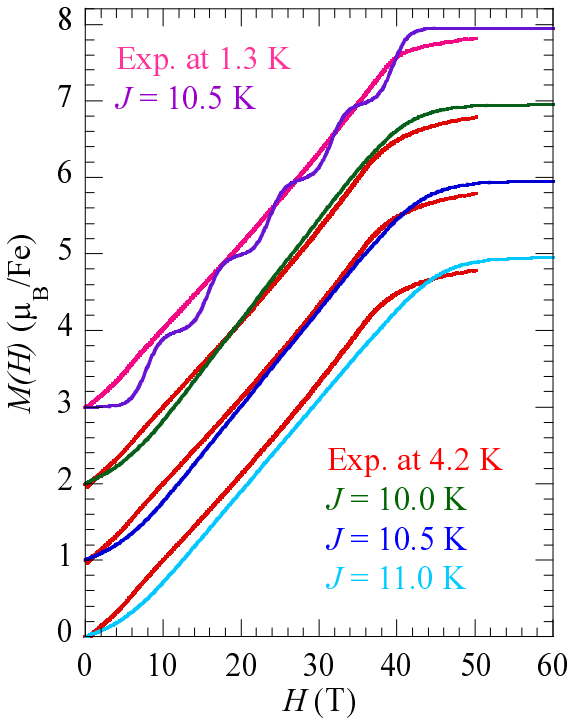

Fig. 4. (Color online) Magnetic-field H dependence of the magnetization $[M(H)]$. The red and pink lines indicate $M(H)$ of the $FeVMoO_7$ powder at 4.2 and 1.3 K, respectively. The three red lines are the same. The green, blue, and lightblue lines indicate $M(H)$ calculated for the isolated AF spin-$\frac{5}{2}$ dimer model at 4.2 K with $J = 10.0$, 10.5, and 11.0 K, respectively. The purple line indicates $M(H)$ calculated for the same model at 1.3 K with $J = 10.5$ K. In the calculation, we used $g = 1.98$ determined in the EPR measurement. The three calculated lines at 4.2 K overlap with one another without vertical shifts. Therefore, the vertical positions of the pairs of experimental and calculated magnetizations are shifted by a step of $1\mu_B$/Fe.

3.2 Neutron diffraction results

The red circles in Fig. 5 indicate the neutron powder diffraction pattern of $FeVMoO_7$ at 15 K above $T_N = 10.8$ K. The wavelength λ is 2.439 Å. We carried out Rietveld refinements using the space group $P\overline{1}$ (No. 2) to evaluate crystal structure parameters. The blue line on the experimental pattern portrays the result of Rietveld refinements and agrees well with the experimental pattern. We show the refined crystal structure parameters in Table II. The atomic positions obtained in this result are similar to those in the literature.[19,20)]

Figure 6(a) shows the neutron powder diffraction pattern of $FeVMoO_7$ at 4 K with the pattern at 15 K from Fig. 5. The two patterns almost overlap each other except for

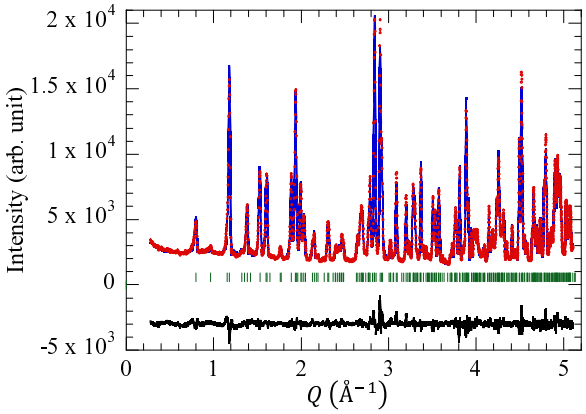

Fig. 5. (Color online) Neutron powder diffraction pattern (red circles) of $FeVMoO_7$ at 15 K. The wavelength λ is 2.439 Å. The blue line on the measured pattern indicates a Rietveld refined pattern obtained using the crystal structure with $P\overline{1}$ (No. 2). The black line at the bottom indicates the difference between the measured and Rietveld refined patterns. The hash marks show the positions of nuclear reflections.

below $Q = 1$ Å^{-1}. We show the difference pattern obtained by subtracting the neutron powder diffraction pattern at 15 K from that at 4 K in Fig. 6(b). We observed several magnetic reflections at 4 K. We can index all the reflections with the propagation vector $(\frac{1}{2}, \frac{1}{2}, \frac{1}{2})$.

We show the T dependence of the integrated intensity of the magnetic reflection at $\frac{1}{2}\frac{1}{2}-\frac{1}{2}$ ($Q = 0.88$ Å^{-1}) in the inset in Fig. 6(b). As T decreases, the intensity increases. We fitted the formula $A(1-\frac{T}{10.8})^{2\beta}$ to the experimental data above 8 K. We obtained $A = 701(90)$ and $\beta = 0.28(3)$.

According to the magnetic space groups in $P\overline{1}$,[24] the allowed magnetic structures are collinear. We carried out Rietveld refinements for the difference pattern using two models. Two ordered moments in each shortest Fe-Fe pair are parallel in one model and antiparallel in the other one. Only the antiparallel model can explain the magnetic reflections as shown in Fig. 6(b).

We show the magnetic structure of $FeVMoO_7$ in Fig. 7(a). An ordered moment vector is $[3.32(5), -0.21(5), 2.15(6)]\mu_B$ lying nearly in the ac plane. Its magnitude is $4.00(7)\mu_B$ at 4 K. Two ordered moments are antiparallel to each other in the shortest Fe-Fe pairs indicated by brown lines, whereas two ordered moments are parallel to each other in the second and third shortest Fe-Fe pairs indicated by green and blue lines, respectively.

Table II. Structural parameters of $FeVMoO_7$ evaluated from Rietveld refinements of the neutron powder diffraction pattern at 15 K. The space group is triclinic $P\overline{1}$ (No. 2). The lattice constants are $a = 5.563(1)$ Å, $b = 6.666(1)$ Å, $c = 7.911(1)$ Å, $\alpha = 96.31(1)°$, $\beta = 90.33(1)°$, and $\gamma = 101.28(1)°$. It is difficult to determine the V position by neutron diffraction experiments because of the small scattering length. We used the position determined by X-ray diffraction .[20] The estimated standard deviations are shown in parentheses. The reliability indexes of the refinement are $R_{\rm p} = 3.81\%$, $R_{\rm wp} = 4.82\%$, and $R_{\rm exp} = 1.83\%$.

Atom	Site	x	y	z	$B_{\rm iso}$ Å^2
Fe	$2i$	0.3265(5)	0.3065(5)	0.4040(3)	0.72(7)
V	$2i$	0.1888	0.7573	0.3342	0.4
Mo	$2i$	0.7959(6)	0.2127(5)	0.1079(4)	0.88(10)
O1	$2i$	0.2957(7)	0.0091(7)	0.3888(5)	0.85(11)
O2	$2i$	0.3936(7)	0.6240(6)	0.4267(5)	0.42(11)
O3	$2i$	0.1660(9)	0.7065(6)	0.1045(5)	0.58(9)
O4	$2i$	0.0860(6)	0.3143(6)	0.5881(4)	0.19(8)
O5	$2i$	0.5643(8)	0.3116(6)	0.2172(5)	1.22(11)
O6	$2i$	0.0690(7)	0.2998(6)	0.2321(4)	0.38(11)
O7	$2i$	0.2775(7)	0.0539(6)	0.9062(5)	0.83(11)

4. Discussion

We consider a probable spin model for $FeVMoO_7$. As described, if the exchange interaction in the shortest Fe-Fe pair is dominant and AF, the spin system consists of AF spin dimers. The spin-$\frac{5}{2}$ on Fe^{3+} ions is usually a Heisenberg spin. Six oxygen ions coordinate octahedrally the Fe^{3+} ion. The symmetries of the crystal fields influencing the Fe^{3+} ions are almost cubic. We infer that the single ion anisotropy of the Fe^{3+} ions is small. Accordingly, we consider the isolated AF Heisenberg spin-$\frac{5}{2}$ dimer model as a first approximation. The Hamiltonian is

$$\mathcal{H} = JS_1 \cdot S_2. \tag{2}$$

Figures 3(b) and 4 show $\chi(T)$ and $M(H)$, respectively, calculated for isolated AF spin-$\frac{5}{2}$ dimers. The calculated $M(H)$ with $J = 10.5$ K is close to the experimental $M(H)$ at 4.2 K. When $J = 10.0$ or 11.0 K, a discrepancy between the calculated and experimental values of $M(H)$ becomes apparent above about 25 T. The calculated $\chi(T)$ with $J = 10.5$ K is also close to the experimental $\chi(T)$ above about 50 K. Consequently, we evaluated J to be 10.5 ± 0.5 K.

We can see, however, a clear difference between the experimental and calculated

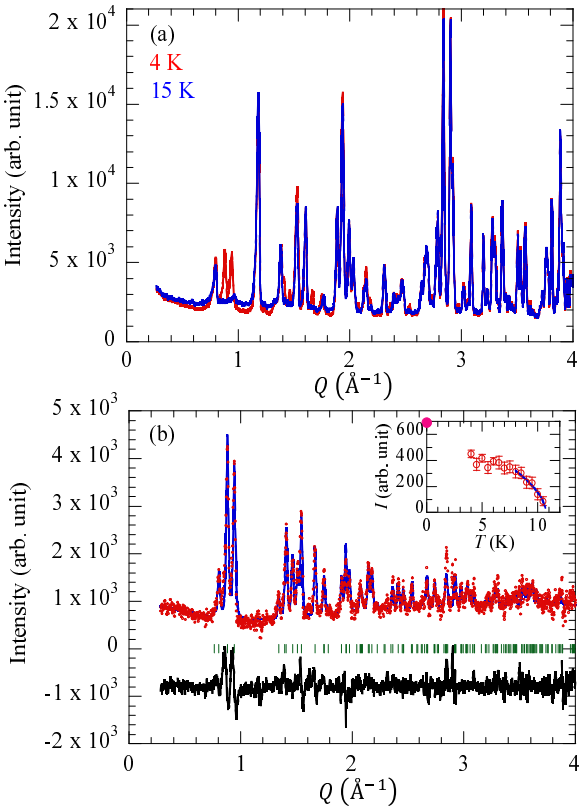

Fig. 6. (Color online) (a) Neutron powder diffraction patterns of $FeVMoO_7$ at 4 and 15 K. The wavelength λ is 2.439 Å. (b) Difference pattern obtained by subtracting the neutron powder diffraction pattern at 15 K from that at 4 K (red circles). The blue line on the measured pattern indicates a Rietveld refined pattern of the magnetic structure only. The black line at the bottom indicates the difference between the measured and Rietveld refined patterns. The hash marks show positions of magnetic reflections. The reliability indexes of the refinement are $R_{\rm p} = 10.3\%$, $R_{\rm wp} = 12.5\%$, and $R_{\rm exp} = 5.56\%$. The inset represents the T dependence of the integrated intensity of the magnetic reflection at $\frac{1}{2}\frac{1}{2} - \frac{1}{2}$ ($Q = 0.88$ Å^{-1}). The blue line shows $A(1 - \frac{T}{T_{\rm N}})^{2\beta}$ with $A = 701$, $T_{\rm N} = 10.8$ K, and $\beta = 0.28$.

$\chi(T)$ at low T. The experimental magnetization at 1.3 K increases monotonically, whereas the calculated one at 1.3 K has magnetization plateaus. We cannot perfectly reproduce $M(H)$ at 4.2 K using the isolated AF spin-$\frac{5}{2}$ dimer model. The discrepancies are probably caused by interdimer interactions that must exist in $FeVMoO_7$ to stabilize the ordered state. Intercluster interactions show a greater effect at lower T in spin cluster compounds.[25–28] Thus, the discrepancies between the experimental and calculated results are apparent at low T.

As described, the isolated AF spin-$\frac{5}{2}$ dimer model can explain the magnetization of $FeVMoO_7$ at 4.2 K but it cannot explain that at 1.3 K. Therefore, we infer that the

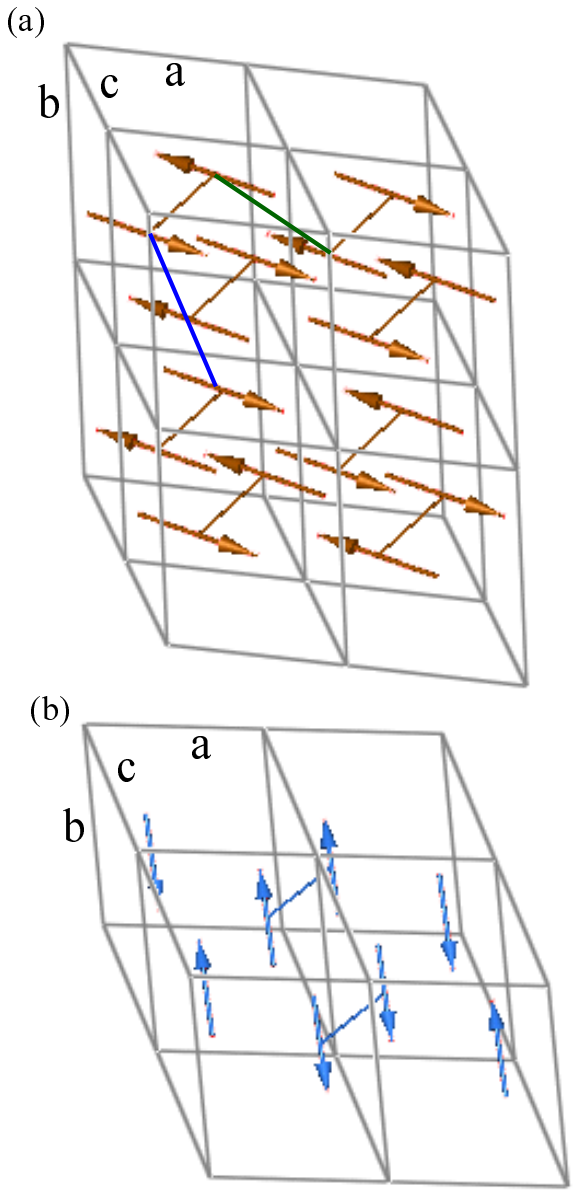

Fig. 7. (Color online) (a) Magnetic structure of $FeVMoO_7$. The brown lines connecting two arrows indicate the shortest Fe-Fe pairs. The green and blue lines indicate the second and third shortest Fe-Fe pairs, respectively. (b) Magnetic structure of $CrVMoO_7$. The lightblue lines connecting two arrows indicate the shortest Cr-Cr pairs.

value of the effective interdimer interaction is close to 4.2 K according to our previous results.[26–28] Here, the effective interdimer interaction is given by the sum of the products of the absolute value of each interdimer interaction ($|J_{\mathrm{int},i}|$) and the corresponding number of interactions per spin (z_i) as $J_{\mathrm{eff}} = \sum_i z_i |J_{\mathrm{int},i}|$. Each $|J_{\mathrm{int},i}|$ must be smaller than 4.2 K. Consequently, we consider that the intradimer interaction (10.5 ± 0.5 K) is

dominant and that the probable spin model is an interacting AF spin-$\frac{5}{2}$ dimer model where spin dimers are connected by interdimer interactions.

On the basis of the following results, we infer that the dominant interdimer interactions are ferromagnetic (F). The experimental $\chi(T)$ is larger than the calculated one at low T. The saturation field is unchanged by the introduction of ferromagnetic interdimer interactions.[29] The neutron-diffraction results indicate that the exchange interactions in the second and third shortest Fe-Fe pairs are ferromagnetic.

In the molecular field theory, $T_{\rm W}$ is given as $S(S+1)zJ/3$, where z is the number of interactions per spin. $T_{\rm W}$ can be larger than J in $S = \frac{5}{2}$ systems. When $J = 10.5$ K and $z = 1$ (dimer), $T_{\rm W}$ is 30.6 K, which is slightly smaller than the experimental value. By taking interdimer interactions into account, the calculated value of $T_{\rm W}$ may be larger than 30.6 K. Similarly, we speculate that $T_{\rm N}$ is close to J because of the large S despite the low-dimensional spin system.

We comment on the β value of $FeVMoO_7$. The β values are 0.36, 0.33, and 1/8 for three-dimensional Heisenberg, three-dimensional Ising, and two-dimensional Ising models, respectively. In the Ising models, β is smaller in the lower dimension. The spin model in $FeVMoO_7$ is an interacting AF spin dimer model (zero-dimensional). Thus, the β value of $FeVMoO_7$ is smaller than that of the three-dimensional Heisenberg models.

The pink circle at 0 K in the inset of Fig. 6(b) indicates the intensity in the case that the magnitude of the moment is the classical value $4.95\mu_{\rm B}$ ($g = 1.98$). The intensity of $FeVMoO_7$ at 0 K cannot reach the intensity indicated by the pink circle. Accordingly, the magnitude of the ordered moment at 0 K is smaller than the classical value $4.95\mu_{\rm B}$ ($g = 1.98$). Since the magnetic Bragg reflections were well reproduced by the collinear spin structure, magnetic frustration on the spin system should be weak. The GS of the isolated spin dimer is a spin-singlet state. Therefore, the ordered moment is reduced by quantum fluctuation.

We have not investigated whether the other possible spin models can explain the experimental results. As shown in Fig. 1(b), an AF-F alternating chain is formed by the exchange interactions in the shortest and second (or third) shortest Fe-Fe pairs. A two-dimensional spin model is formed by the three types of exchange interactions. We do not have susceptibility and magnetization results calculated for the spin models. In future, if we can make large single crystals and investigate magnetic excitations using inelastic neutron scattering, we can precisely estimate the spin model for $FeVMoO_7$. Then we will compare the experimental results with those calculated for the estimated

spin model.

We compare the magnetic structure of $FeVMoO_7$ with that of isostructural $CrVMoO_7$ shown in Fig. 7(b). The magnetic structure shown here is the same as that reported in the literature.[27] The propagation vector is $(\frac{1}{2}, 0, \frac{1}{2})$, which is different from the propagation vector $(\frac{1}{2}, \frac{1}{2}, \frac{1}{2})$ in $FeVMoO_7$. An ordered moment vector in $CrVMoO_7$ is $[0.10(5), 2.41(4), -1.42(6)]\mu_B$ lying nearly in the *bc* plane.[30] Its magnitude is $2.92(7)\mu_B$. The ordered moment vector is 4 times larger than that reported in the literature[27] because of a mistake in the scale factor. Two ordered moments are aligned in parallel and antiparallel in the shortest Cr-Cr and Fe-Fe pairs indicated by lines, respectively. The report of the antiparallel alignment of two ordered moments in the shortest Cr-Cr pair[27] is incorrect. The ellipse in Fig. 7 in the literature[27] indicates the second shortest Cr-Cr pair. The magnetism of $CrVMoO_7$ can be explained well by the interacting antiferromagnetic spin-$\frac{3}{2}$ dimer model. The dominant AF interaction may exist in the second shortest Cr-Cr pairs (4.97 Å) or in the third shortest pairs (5.24 Å).

We consider the origin of the sign of the exchange interactions. The exchange interactions are AF (F), F (AF), and F (AF) in the shortest, second shortest, and third shortest Fe-Fe (Cr-Cr) pairs, respectively. An exchange interaction is the sum of direct exchange and superexchange interactions. The midpoint of two Fe (or Cr) ions in the shortest pair is an inversion center of the crystal structure. 3*d* orbits of the two Fe (or Cr) ions are expected to overlap each other. The direct exchange interactions are probably AF. The Fe-O-Fe and Cr-O-Cr angles in the shortest pair are 100° and 99°, respectively. The superexchange interactions are probably F. We speculate that the sum of the AF and F interactions results in the weak AF and F interactions in the shortest pairs of $FeVMoO_7$ and $CrVMoO_7$, respectively. We do not know which paths are dominant for the interactions in the second and third shortest pairs. Therefore, we do not know the origin of the signs of the interactions.

5. Conclusion

We studied the magnetism of $FeVMoO_7$ by performing magnetization, specific heat, electron spin resonance (ESR), and neutron diffraction experiments. We observed an antiferromagnetically ordered state below $T_N = 10.8$ K. The broad maximum of magnetic susceptibility around 16 K indicates a low-dimensional AF spin system with short-range correlations. The magnetization increases monotonically with increasing magnetic field and seems to approach saturation above 40 T. We consider that the probable spin

model is an interacting antiferromagnetic spin-$\frac{5}{2}$ dimer model where spin dimers are connected by interdimer interactions. We evaluated the intradimer interaction J to be 10.5 ± 0.5 K. We determined the magnetic structure. Two ordered magnetic moments are antiparallel in each dimer (shortest Fe-Fe pair). The magnitude of the moments is $4.00(7)\mu_{\mathrm{B}}$ at 4 K. The magnitude at 0 K is considered to be smaller than the classical value $4.95\mu_{\mathrm{B}}$ ($g = 1.98$ determined in the ESR measurements). We confirmed the reduction of ordered magnetic moments by quantum fluctuation in high-spin (spin-$\frac{5}{2}$) clusters as known in high-spin chains.

Acknowledgments

This work was financially supported by Japan Society for the Promotion of Science (JSPS) KAKENHI (Grant Nos. 15K05150 and 18K03551), grants from National Institute for Materials Science (NIMS), and Development of advanced hydrogen liquefaction system by using magnetic refrigeration technology, Japan Science and Technology Agency (JST). The high-field magnetization experiments were conducted under the Visiting Researcher's Program of the Institute for Solid State Physics (ISSP), The University of Tokyo. The neutron powder diffraction experiments were performed by using the ECHIDNA diffractometer at Australian Nuclear Science and Technology Organisation (ANSTO), Australia (proposal ID. MI7075). We are grateful to M. Matsumoto for the fruitful discussion, to S. Matsumoto for the sample syntheses and X-ray diffraction measurements, and to T. Furubayashi for the ESR measurements.

References

1) M. Hase, I. Terasaki, and K. Uchinokura, Phys. Rev. Lett. **70**, 3651 (1993).

2) M. Hase, I. Terasaki, Y. Sasago, K. Uchinokura, and H. Obara, Phys. Rev. Lett. **71**, 4059 (1993).

3) M. Hase, I. Terasaki, K. Uchinokura, M. Tokunaga, N. Miura, and H. Obara, Phys. Rev. B **48**, 9616 (1993).

4) F. D. M. Haldane, Phys. Lett. A **93**, 464 (1983).

5) F. D. M. Haldane, Phys. Rev. Lett. **50**, 1153 (1983).

6) I. Affleck, T. Kennedy, E. H. Lieb, and H. Tasaki, Commun. Math. Phys. **115**, 477 (1988).

7) T. Yang, Y. Zhang, S. Yang, G. Li, M. Xiong, F. Liao, and J. Lin, Inorg. Chem. **47**, 2562 (2008).

8) M. Hase, T. Yang, R. Cong, J. Lin, A. Matsuo, K. Kindo, K. Ozawa, and H. Kitazawa, Phys. Rev B **80**, 054402 (2009).

9) M. Hase, V. Yu. Pomjakushin, L. Keller, A. Dönni, O. Sakai, T. Yang, R. Cong, J. Lin, K. Ozawa, and H. Kitazawa, Phys. Rev B **84**, 184435 (2011).

10) M. Hase, M. Matsuda, K. Kaneko, N. Metoki, K. Kakurai, T. Yang, R. Cong, J. Lin, K. Ozawa, and H. Kitazawa, Phys. Rev B **84**, 214402 (2011).

11) M. Hase, V. Yu. Pomjakushin, A. Dönni, T. Yang, R. Cong, and J. Lin, J. Phys. Soc. Jpn. **83**, 104701 (2014).

12) L. D. Sanjeewa, V. O. Garlea, M. A. McGuire, C. D. McMillen, H. Cao, and J. W. Kolis, Phys. Rev. B **93**, 224407 (2016).

13) J. Ma, C. D. Dela Cruz, T. Hong, W. Tian, A. A. Aczel, S. Chi, J.-Q. Yan, Z. L. Dun, H. D. Zhou, and M. Matsuda, Phys. Rev. B **88**, 144405 (2013).

14) A. K. Bera, B. Lake, W.-D. Stein, and S. Zander, Phys. Rev. B **89**, 094402 (2014).

15) G. J. Redhammer, A. Senyshyn, M. Meven, G. Roth, S. Prinz, A. Pachler, G. Tippelt, C. Pietzonka, W. Treutmann, M. Hoelzel, B. Pedersen, and G. Amthauer, Phys. Chem. Miner. **38**, 139 (2011).

16) G. J. Redhammer, G. Roth, W. Treutmann, M. Hoelzel, W. Paulus, G. André, C. Pietzonka, and G. Amthauer, J. Solid State Chem. **182**, 2374 (2009).

17) M. Matsumoto, H. Kuroe, T. Sekine, and T. Masuda, J. Phys. Soc. Jpn. **79**, 084703 (2010).

18) T. Masuda, A. Zheludev, B. Grenier, S. Imai, K. Uchinokura, E. Ressouche, and S. Park, Phys. Rev. Lett. **93**, 077202 (2004).

19) A. Le Bail, L. Permér, and Y. Laligant, Eur. J. Solid State Inorg. Chem. **32**, 883 (1995).

20) X. Wang, K. R. Heier, C. L. Stern, and K. R. Poeppelmeier, Inorg. Chem. **37**, 3252 (1998).

21) J. Rodriguez-Carvajal, Physica B **192**, 55 (1993); [http://www.ill.eu/sites/fullprof/].

22) T. Groń, J. Krok-Kowalski, M. Kurzawa, and J. Walczak, J. Magn. Magn. Mater. **101**, 148 (1991).

23) M. Kurzawa, J. Mater. Sci. **27**, 1361 (1992).

24) D. B. Litvin, Acta Crystallogr. A **64**, 419 (2008).

25) M. Hase, K. Nakajima, S. Ohira-Kawamura, Y. Kawakita, T. Kikuchi, and M. Matsumoto, Phys. Rev B **92**, 184412 (2015).

26) M. Hase, M. Matsumoto, A. Matsuo, and K. Kindo, Phys. Rev. B **94**, 174421 (2016).

27) M. Hase, Y. Ebukuro, H. Kuroe, M. Matsumoto, A. Matsuo, K. Kindo, J. R. Hester, T. J. Sato, and H. Yamazaki, Phys. Rev. B **95**, 144429 (2017).

28) M. Hase, A. Matsuo, K. Kindo, and M. Matsumoto, Phys. Rev. B **96**, 214424 (2017).

29) M. Matsumoto, private communication.

30) M. Hase, Y. Ebukuro, H. Kuroe, M. Matsumoto, A. Matsuo, K. Kindo, J. R. Hester, T. J. Sato, and H. Yamazaki, Phys. Rev. B **98**, 139901(E) (2018).